Control of Spin State in (Porphinato)iron(III) Complexes. An Axial Ligand Orientation Effect on the Spin State in Bis(2-methylimidazole)(octaethylporphinato)iron(III) Perchlorate

David K. Geiger, Young Ja Lee, and W. Robert Scheidt*

Contribution from the Department of Chemistry, University of Notre Dame, Notre Dame, Indiana 46556. *Received March 5, 1984*

Abstract: The preparation of the six-coordinate complex bis(2-methylimidazole)(octaethylporphinato)iron(III) perchlorate is described. The molecule has been characterized by magnetic susceptibilities (solution and state solid), electron paramagnetic resonance, and a crystal structure determination. In solution, the complex has magnetic properties consistent with a thermal spin equilibrium ($S = {}^1/_2 \rightleftarrows S = {}^5/_2$). In the solid, the magnetic data are consistent with a spin admixed system with predominant $S = {}^5/_2$ character. At room temperature, $\mu = 5.52\ \mu_B$. The crystal structure analysis leads to the suggestion that the state-dependent magnetic properties are a result of the axial ligand orientation, e.g., the orientation of the axial ligands with respect to the equatorial Fe–N_p bond vectors. In the solid state, the projection of the 2-MeIm ligand plane onto the porphinato core of the centrosymmetric complex is within 22° of eclipsing opposite Fe–N_p bonds. Thus, steric hindrance between axial ligand atoms and the porphinato core does not permit the short axial bond required to achieve a low-spin state. In solution, freer rotation around the axial Fe–N bonds is expected, and consequently the shorter axial Fe–N(2-MeIm) bonds appropriate for a low-spin state can be realized. Crystal data: triclinic, space group $P\bar{1}$, $a = 10.274$ (1) Å, $b = 12.276$ (2) Å, $c = 9.038$ (2) Å, $\alpha = 91.60$ (1)°, $\beta = 109.38$ (1)°, and $\gamma = 88.71$ (1)°, $Z = 1$, and molecular formula $FeClO_4N_8C_{44}H_{56}$. The structure is based on 7692 reflections measured on an automated diffractometer to $(\sin\theta)/\lambda \leq 0.817$ Å^{-1}. Final discrepancy indices are $R_1 = 0.046$ and $R_2 = 0.063$. Pertinent structural parameters include a radially expanded core with Fe–N_p = 2.041 Å and an axial Fe–N distance of 2.275 Å.

A major objective in current synthetic and structural studies of iron porphyrinate complexes has been to achieve an understanding of the control of the spin state of iron.[1,2] A primary determinant of the spin state is the nature and number of the axial ligands.[1] The nature of the porphinato ligand can also play a role.[3] Subtler effects may also be important. A number of hemoproteins which display thermal spin equilibria between a high-spin and a low-spin state also show quantitative differences in the spin equilibrium,[4] even though there is nominal parity in ligation of the iron atom. What features of the hemoprotein could mediate such effects? Coordination chemists would be inclined to look for mechanisms by which the protein could qualitatively change the nature of the axial ligand interactions. One suggestion has been hydrogen bonding by a protein residue to the axial ligand.[5] We would like to suggest that the rotational orientation of the axial ligand(s) can also play a role.

We have recently characterized two crystalline forms of [Fe(OEP)(3-Clpy)$_2$]ClO_4.[6] A triclinic form[7] displays a thermal (high to low) spin equilibrium,[8] while the monoclinic form[9] is an intermediate-spin complex. We ascribed[9] the striking differences in the electronic structure of these two solid-state forms of the molecule to a ligand orientation effect. The ligand orientation simply refers to the orientation of the axial ligand plane projected onto the equatorial porphyrin plane (Figure 1). The ligand plane orientation in the two forms of the molecule is controlled by solid-state packing effects. A ~31° rotation of the 3-chloropyridine plane around the axial Fe–N bonds appears to control whether or not the low-spin state is accessible. In both complexes, the two axial pyridine rings are effectively coplanar. In the triclinic form, ϕ is 41° and the axial bond distances can readily vary over the ~0.3-Å difference appropriate for the high- and low-spin states.[1] In the monoclinic form, the average ϕ value is 9.5°, and the 2.00-Å axial bond distance appropriate for the low-spin state cannot be achieved because of nonbonded repulsions between the axial ligand and the porphinato core. With the low-spin state thus inhibited, an intermediate spin state, sterically acceptable for the ligand orientation, results. Control of axial ligand orientation would seem to be a sufficiently low-energy process to be readily modulated by protein structure. We thus felt that further, systematic, study of axial ligand orientation effects on spin state was warranted.

Controlling the axial ligand orientation in a relatively simple metalloporphyrin complex presents some difficulties. For example, the use of a covalently attached axial ligand or "tailed" porphyrin has, in two instances,[10] yielded a solid-state species with significantly different axial ligand orientations than would be suggested from inspection of scaled molecular models.[11] A more constrained

(1) Scheidt, W. R.; Reed, C. A. *Chem. Rev.* **1981**, *81*, 543–555.
(2) Scheidt, W. R.; Gouterman, M. In "Physical Bioinorganic Chemistry—Iron Porphyrins, Part I"; Lever, A. B. P., Gray, H. B., Eds.; Addison-Wesley: Reading, MA, 1983; pp 89–139.
(3) Geiger, D. K.; Scheidt, W. R. *Inorg. Chem.* **1984**, *23*, 1970–1972.
(4) Beetlestone, J.; George, P. *Biochemistry* **1964**, *3*, 707–714. Iizuka, T.; Kotani, M. *Biochim. Biophys. Acta* **1968**, *154*, 417–419; *Ibid.* **1969**, *181*, 275–286; *Ibid.* **1969**, *194*, 351–363. Anusiem, A. C. I.; Kelleher, M. *Biopolymers* **1978**, *17*, 2047–2055. Perutz, M. F.; Sanders, J. K. M.; Chenery, D. H.; Noble, R. W.; Pennelly, R. R.; Fund, L. W.-M.; Ho, C.; Biannini, I.; Porschke, D.; Winkler, H. *Biochemistry* **1978**, *17*, 3640–3652. Messana, C.; Cerdonio, M.; Shenkin, P.; Noble, R. W.; Fermi, G.; Perutz, R. W.; Perutz, M. F. *Ibid.* **1978**, *717*, 3652–3662. Sligar, S. G. *Ibid.* **1976**, *15*, 5399–5406. Lange, R.; Bonfils, C.; Debye, P. *Eur. J. Biochem.* **1977**, *79*, 623–628. Yonetani, T.; Iizuka, T.; Asakura, T. *J. Biol. Chem.* **1972**, *247*, 863–868.
(5) Valentine, J. S.; Sheridan, R. P.; Allen, L. C.; Kahn, P. C. *Proc. Natl. Acad. Sci. U.S.A.* **1979**, *76*, 1009–1013. Quinn, R.; Strouse, C. E.; Valentine, J. S. *Inorg. Chem.* **1983**, *22*, 3934–3940 and references cited therein.
(6) Abbreviations: OEP, TPP, PPIX, the dianions of octaethylporphyrin, *meso*-tetraphenylporphyrin, and protoporphyrin IX, respectively; 3-Clpy, 3-chloropyridine; py, pyridine; 2-$MeIm_2$, 2-methylimidazole; 1-MeIm, 1-methylimidazole; HIm, imidazole; BzIm, benzimidazole; N_p, porphinato nitrogen atom.
(7) Scheidt, W. R.; Geiger, D. K.; Haller, K. J. *J. Am. Chem. Soc.* **1982**, *104*, 495–499.
(8) Hill, H. A. O.; Skyte, P. D.; Buchler, J. W.; Lueken, H.; Tonn, M.; Gregson, A. K.; Pellizer, G. *J. Chem. Soc., Chem. Commun.* **1979**, *151*–152. Gregson, A. K. *Inorg. Chem.* **1981**, *20*, 81–87.
(9) Scheidt, W. R.; Geiger, D. K.; Hayes, R. G.; Lang, G. *J. Am. Chem. Soc.* **1983**, *105*, 2625–2632.
(10) Mashiko, T.; Reed, C. A.; Haller, K. J.; Kastner, M. E.; Scheidt, W. R. *J. Am. Chem. Soc.* **1981**, *103*, 5758–5767. Bobrik, M. A.; Walker, F. A. *Inorg. Chem.* **1980**, *19*, 3383–3390.
(11) CPK models of the entire complex are used. In these two complexes, it was expected that the length of the covalent linkage would lead to the ligand plane being between porphinato nitrogen atoms. However, the observed orientations are much more nearly over porphinato nitrogen atoms.

0002-7863/84/1506-6339$01.50/0 © 1984 American Chemical Society

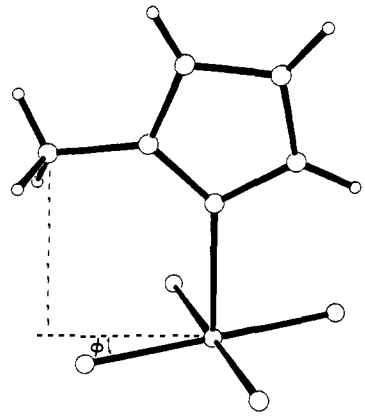

Figure 1. Diagram illustrating the definition of the angle ϕ as a way of specifying the axial ligand plane orientation. Also shown in the figure is the observed orientation of the methyl group hydrogen atoms of the axial ligands in $[Fe(OEP)(2\text{-MeIm})_2]ClO_4$.

ligand system, on the other hand, might well be insufficiently flexible to allow structures appropriate[1] for all possible spin states. Our approach was to synthesize bisligated ferric porphyrinates in which the axial ligands have modest steric bulk. Only modest steric bulk can be allowed to permit the possibility of attaining the geometry appropriate for any of the possible spin states. We have prepared and characterized the complex bis(2-methylimidazole)(octaethylporphinato)iron(III) perchlorate, $[Fe(OEP)(2\text{-MeIm})_2]ClO_4$. This complex has a near high-spin state in the solid but significantly lower (and temperature dependent) magnetic moments in solution. The X-ray structure determination of $[Fe(OEP)(2\text{-MeIm})_2]ClO_4$ along with structural data for other porphinato species suggests that these differences in magnetic properties could arise from axial ligand orientation effects.

Experimental Section

Synthesis and Physical Data. $[Fe(OEP)OClO_3]$ was prepared by the method of Dolphin et al.[12] $[Fe(OEP)(2\text{-MeIm})_2]ClO_4$ was prepared by dissolving 50 mg (0.073 mmol) of $[Fe(OEP)OClO_3]$ in 7 mL of chloroform that was 50 mM in 2-methylimidazole. Rectangular blocks of $[Fe(OEP)(2\text{-MeIm})_2]ClO_4$ were formed in essentially quantitative yield by allowing hexane to diffuse into the solution. Solution magnetic susceptibilities were determined as a function of temperature by the method of Evans[13] and were corrected for changes in solvent density.[14] Measurements were made in $CDCl_3$ solution that contained approximately a 50-fold excess of 2-methylimidazole and 2% Me_4Si by using a Varian XL-100 NMR spectrometer. The probe temperature was monitored with an iron–constantin thermocouple. A diamagnetic correction of -704×10^{-6} cgs/mol was used for OEP; Pascal's constants[15] were used for the remaining constituents (total correction -832×10^{-6} cgs/mol). A marked temperature dependence was observed in solution: 309 K, 3.45 μ_B; 303 K, 3.22 μ_B; 275 K, 2.83 μ_B; 261 K, 2.75 μ_B; 230 K, 2.63 μ_B.

The magnetic susceptibility of the complex was also determined in the solid state over the temperature range 6.0–321 K on a SHE SQUID susceptometer courtesy of Prof. C. A. Reed. The results are shown in Figure 2. The room temperature moment is 5.54 μ_B. The EPR of $[Fe(OEP)(2\text{-MeIm})_2]ClO_4$ was also examined in the solid state at 77 K; an axial spectrum with $g_\perp = 5.41$ and $g_\parallel = 1.976$ was observed.

X-ray Structure Determination. Preliminary examination of a crystal of $[Fe(OEP)(2\text{-MeIm})_2]ClO_4$ with dimensions of $0.33 \times 0.45 \times 0.50$ mm on a Nicolet $P\bar{1}$ diffractometer established a one-molecule triclinic unit cell, space group $P1$ or $P\bar{1}$. Cell constants ($\bar{\lambda}$ 0.710 73 Å) came from a least-squares refinement of 60 automatically centered reflections, at $\pm 2\theta$, and are $a = 10.274$ (1) Å, $b = 12.276$ (2) Å, $c = 9.038$ (2) Å, $\alpha = 91.60$ (1)°, $\beta = 109.38$ (1)°, and $\gamma = 88.71$ (1)°. A Delauney reduction revealed no hidden symmetry. The calculated density was 1.317 g/cm^3 for a cell content of $[Fe(OEP)(2\text{-MeIm})_2]ClO_4$; the experimental density is 1.31 g/cm^3. All measurements were made at the ambient laboratory temperature of 19 ± 1 °C.

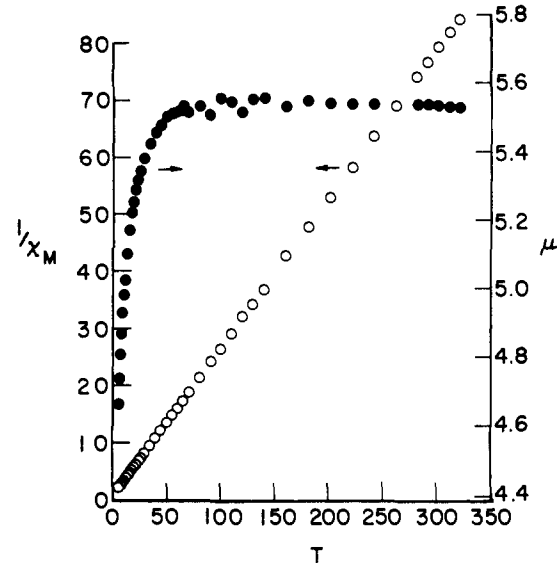

Figure 2. Plot of $1/\chi_m$ vs. T and μ_B vs. T for $[Fe(OEP)(2\text{-MeIm})_2]ClO_4$.

Intensity data were measured at 19 °C by using graphite-monochromated Mo Kα radiation and θ–2θ scanning. Variable 2θ scans (2–12 deg/min) with scans of 0.5° below and above Kα_1 and Kα_2 and backgrounds at the extremes of the scan (for 0.5 times the time required for the scan) were employed. All independent data to $(\sin\theta/\lambda \leq 0.817$ Å^{-1} were measured. Measurement of four standard relections throughout data collection (every 50 reflections) show no trends with exposure to the X-ray beam. Net intensities were reduced as described previously.[16] No absorption correction was deemed necessary ($\mu = 0.461$ mm^{-1}). Reflections having $F_o > 3\sigma(F_o)$ were considered observed. A total of 7692 unique data, 79% of the theoretical number possible, were used in the subsequent solution and refinement of structure.

The structure was solved in the centrosymmetric space group $P\bar{1}$ with the direct methods program MULTAN78.[17] The choice of space group was confirmed by all subsequent developments in the structure solution and refinement. Most atoms of the complex were found in the E map. The remaining atoms of the complex and a disordered perchlorate ion (at an inversion center $^1/_2$, 0, 0) were found in subsequent difference Fourier syntheses. After several cycles of full-matrix least-squares refinement, a difference Fourier map revealed the approximate positions of all hydrogen atoms. The hydrogen atoms were included in all subsequent cycles of least squares as fixed contributors (C–H = 0.95 Å, N–H = 0.87 Å, and $B(H) = B(C \text{ or } N) + 1.0$ Å^2). Least-squares refinement was then carried to convergence for the 283 variables, which included anisotropic temperature factors for all heavy atoms. At convergence, final values for the discrepancy indices were $R_1 = 0.046$ and $R_2 = 0.063$[18] with a final data/parameter ratio of 27.2 and an error of fit of 1.83. A final difference Fourier was essentially featureless with the highest peak of 0.61 e/Å^3 near O(2) and O(3) of the perchlorate ion and smaller peaks (<0.33 e/Å^3) elsewhere in the map. Final atomic coordinates are listed in Table I. Tables II and III, tables of anisotrpic temperature factors and fixed hydrogen atom coordinates, are available as supplementary material.

Results and Discussion

The temperature-dependent magnetic susceptibility of solid $[Fe(OEP)(2\text{-MeIm})_2ClO_4$ (Figure 2) is in general form that expected for a high-spin iron(III) porphyrinate with a large zero-field splitting.[19] However, the magnetic momement per iron

(12) Dolphin, D. H.; Sams, J. R.; Tsin, T. B. *Inorg. Chem.* **1977**, *16*, 711–713.
(13) Evans, D. F. *J. Chem. Soc.* **1959**, 2003–2005.
(14) Ostfeld, D.; Cohen, I. A. *J. Chem. Ed.* **1972**, *49*, 829. Washburn, E. W., Ed. "International Critical Tables"; McGraw-Hill: New York, 1929; Vol. III, p 28.
(15) Mulay, L. N. In "Physical Methods of Chemistry"; Weissburger, A., Rossiter, R., Eds.; Wiley-Interscience: New York, 1972; Vol. I, part IV.
(16) Scheidt, W. R. *J. Am. Chem. Soc.* **1974**, *96*, 84–89.
(17) Programs used in this study included local modifications of Main, Hull, Lessinger, Germain, Declerq, and Woolfson's MULTAN78, Jacobson's ALFF and ALLS, Busing and Levy's ORFFE and ORFLS, and Johnson's ORTEP2. Atomic form factors were from: Cromer, D. T.; Mann, J. B. *Acta Crystallogr., Sect. A* **1968**, *A24*, 321–323. Real and imaginary corrections for anomalous dispersion in the form factor of the iron and chlorine atoms were from: Cromer, D. T.; Liberman, D. J. *J. Chem. Phys.* **1970**, *53*, 1891–1898. Scattering factors for hydrogen were from: Stewart, R. F.; Davidson, E. R.; Simpson, W. T. *Ibid.* **1965**, *42*, 3175–3187.
(18) $R_1 = \sum||F_o| - |F_c||/\sum|F_o|$ and $R_2 = [\sum w(|F_o| - |F_c|)^2/\sum w(F_o)^2]^{1/2}$.
(19) Mitra, S. In "Physical Bioinorganic Chemistry—Iron Porphyrins, Part II"; Lever, A. B. P., Gray, H. B., Eds.; Addison-Wesley: Reading, MA, 1983; pp 1–42.

Table I. Fractional Coordinates in the Unit Cell[a]

atom	*x*	*y*	*z*
Fe	0.0	0.0	0.0
Cl	0.5000	0.5000	0.0
N(1)	0.138 11 (11)	0.089 15 (8)	0.175 10 (12)
N(2)	0.019 68 (11)	0.105 95 (8)	−0.159 97 (12)
N(3)	−0.183 20 (11)	0.094 49 (9)	0.029 47 (13)
N(4)	−0.347 84 (14)	0.209 82 (11)	0.033 61 (17)
O(1)	0.465 5 (3)	0.395 72 (22)	0.015 5 (5)
O(2)	0.414 1 (4)	0.555 5 (4)	−0.118 7 (7)
O(3)	0.511 8 (5)	0.566 3 (5)	0.144 9 (8)
O(4)	0.639 1 (3)	0.500 14 (29)	−0.007 5 (5)
C(a1)	0.183 49 (12)	0.066 85 (10)	0.332 25 (14)
C(a2)	0.206 70 (13)	0.180 55 (10)	0.158 77 (15)
C(a3)	0.100 78 (13)	0.197 23 (10)	−0.130 73 (15)
C(a4)	−0.051 90 (13)	0.103 23 (10)	−0.318 59 (14)
C(b1)	0.282 03 (13)	0.148 15 (11)	0.418 70 (15)
C(b2)	0.297 27 (13)	0.218 08 (11)	0.310 34 (16)
C(b3)	0.077 00 (14)	0.255 29 (10)	−0.274 62 (16)
C(b4)	−0.017 93 (14)	0.197 13 (10)	−0.390 90 (15)
C(m1)	0.143 11 (13)	−0.022 07 (10)	0.397 72 (15)
C(m2)	0.189 34 (13)	0.229 81 (10)	0.015 89 (16)
C(1)	−0.230 57 (15)	0.195 68 (11)	0.000 36 (18)
C(2)	−0.378 63 (17)	0.114 46 (14)	0.086 88 (22)
C(3)	−0.277 24 (16)	0.044 01 (12)	0.083 35 (19)
C(4)	−0.168 92 (25)	0.286 06 (14)	−0.058 2 (3)
C(11)	0.352 88 (17)	0.151 92 (13)	0.593 91 (17)
C(12)	0.485 03 (24)	0.087 35 (23)	0.650 09 (24)
C(21)	0.386 03 (16)	0.317 38 (13)	0.339 57 (19)
C(22)	0.308 82 (28)	0.421 86 (16)	0.347 8 (3)
C(31)	0.138 82 (17)	0.362 26 (12)	−0.287 37 (19)
C(32)	0.065 52 (25)	0.458 04 (15)	−0.239 1 (3)
C(41)	−0.086 28 (17)	0.229 32 (13)	−0.558 25 (17)
C(42)	−0.218 69 (24)	0.293 05 (19)	−0.577 37 (23)

[a] The estimated standard deviations of the least significant digits are given in parentheses.

Table IV. Bond Lengths in $[Fe(OEP)(2\text{-}MeIm)_2]ClO_4$[a]

type	length, Å	type	length, Å
Fe–N(1)	2.049 (1)	C(b3)–C(b4)	1.369 (2)
Fe–N(2)	2.033 (1)	C(1)–N(4)	1.342 (2)
Fe–N(3)	2.275 (1)	C(1)–C(4)	1.483 (2)
N(1)–C(a1)	1.373 (2)	C(2)–N(4)	1.361 (2)
N(1)–C(a2)	1.375 (2)	C(2)–C(3)	1.347 (2)
N(2)–C(a3)	1.378 (2)	C(11)–C(b1)	1.507 (2)
N(2)–C(a4)	1.377 (2)	C(11)–C(12)	1.499 (3)
N(3)–C(1)	1.325 (2)	C(21)–C(b2)	1.503 (2)
N(3)–C(3)	1.382 (2)	C(21)–C(22)	1.506 (3)
C(a1)–C(b1)	1.452 (2)	C(31)–C(b3)	1.495 (2)
C(a1)–C(m1)	1.390 (2)	C(31)–C(32)	1.513 (3)
C(a2)–C(b2)	1.447 (2)	C(41)–C(b4)	1.501 (2)
C(a2)–C(m2)	1.397 (2)	C(41)–C(42)	1.515 (3)
C(a3)–C(b3)	1.446 (2)	Cl–O(1)	1.359 (3)
C(a3)–C(m2)	1.389 (2)	Cl–O(2)	1.334 (4)
C(a4)–C(b4)	1.445 (2)	Cl–O(3)	1.494 (5)
C(a4)–C(m1)′	1.393 (2)	Cl–O(4)	1.453 (3)
C(b1)–C(b2)	1.369 (2)		

[a] The numbers in parentheses are the estimated standard deviations. Primed and unprimed atoms are related by the center of inversion.

atom is 5.54 μ_B at room temperature, lower than the expected 5.92 μ_B for a pure $S = {}^5/_2$ state. This lower value might arise from a thermal spin equilibrium or a quantum mechanically admixed ground state. The constant value of the moment above about 60 K is inconsistent with a thermal spin equilibrium in the solid state, unlike the solution magnetic moments. The best description would appear to be that of a quantum mechanically admixed ground state, which is predominantly $S = {}^5/_2$ with some close-lying $S = {}^3/_2$ state mixed in. The general magnetic behavior in the solid is similar to that observed[20] for $[Fe(TPP)(C_2H_5OH)_2]ClO_4 \cdot {}^1/_2CH_2Cl_2$. The general character of the EPR spectrum, e.g., an axial spectrum with $g_\perp < 6$, is consistent with an admixed ground

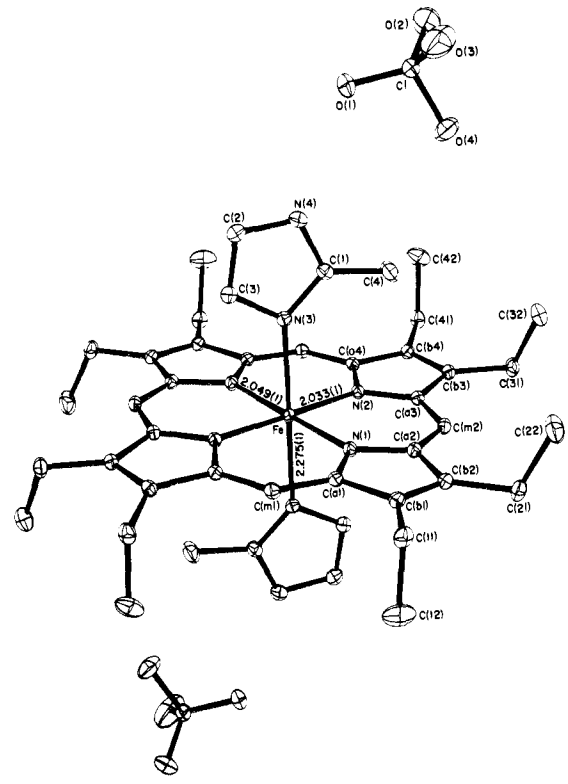

Figure 3. Computer-drawn model, in perspective, of $[Fe(OEP)(2\text{-}MeIm)_2]ClO_4$. The labels for all crystallographically unique atoms of the molecule are displayed. 55% probability ellipsoids are drawn for all atoms.

Table V. Bond Angles in $[Fe(OEP)(2\text{-}MeIm)_2]ClO_4$[a]

angle	value, deg	angle	value, deg
N(1)FeN(2)	89.58 (4)	C(b4)C(b3)C(31)	127.79 (12)
N(1)FeN(3)	92.28 (4)	C(a4)C(b4)C(b3)	106.94 (11)
N(2)FeN(3)	92.36 (4)	C(a4)C(b4)C(41)	125.58 (12)
C(a1)N(1)C(a2)	106.48 (10)	C(b3)C(b4)C(41)	127.18 (12)
C(a3)N(2)C(a4)	106.61 (10)	C(a1)C(m1)C(a4)′	127.01 (12)
C(1)N(3)C(3)	105.04 (12)	C(a2)C(m2)C(a3)	126.72 (12)
C(1)N(4)C(2)	108.68 (12)	N(3)C(1)N(4)	110.47 (13)
N(1)C(a1)C(b1)	109.97 (11)	N(3)C(1)C(4)	128.05 (14)
N(1)C(a1)C(m1)	124.76 (11)	N(4)C(1)C(4)	121.48 (13)
C(b1)C(a1)C(m1)	125.25 (12)	N(4)C(2)C(3)	105.41 (13)
N(1)C(a2)C(b2)	110.16 (11)	N(3)C(3)C(2)	110.40 (13)
N(1)C(a2)C(m2)	124.38 (11)	C(b1)C(11)C(12)	114.66 (15)
C(b2)C(a2)C(m2)	125.46 (12)	C(b2)C(21)C(22)	113.41 (15)
N(2)C(a3)C(b3)	109.79 (11)	C(b3)C(31)C(32)	112.81 (14)
N(2)C(a3)C(m2)	124.94 (11)	C(b4)C(41)C(42)	110.95 (14)
C(b3)C(a3)C(m2)	125.25 (12)	FeN(1)C(a1)	126.34 (8)
N(2)C(a4)C(b4)	109.8 (11)	FeN(2)C(a2)	127.15 (8)
N(2)C(a4)C(m1)′	125.15 (11)	FeN(2)C(a3)	127.12 (8)
C(b4)C(a4)C(m1)	125.04 (12)	FeN(2)C(a4)	126.19 (8)
C(a1)C(b1)C(b2)	106.67 (11)	FeN(3)C(1)	134.15 (10)
C(a1)C(b1)C(11)	125.53 (12)	FeN(3)C(3)	120.76 (9)
C(b2)C(b1)C(11)	127.80 (12)	O(1)ClO(2)	116.72 (24)
C(a2)C(b2)C(b1)	106.71 (11)	O(1)ClO(3)	110.76 (27)
C(a2)C(b2)C(21)	125.44 (12)	O(1)ClO(4)	108.80 (19)
C(b1)C(b2)C(21)	127.82 (12)	O(2)ClO(3)	105.9 (3)
C(a3)C(b3)C(b4)	106.83 (11)	O(2)ClO(4)	110.38 (26)
C(a3)C(b3)C(31)	125.26 (12)	O(3)ClO(4)	103.45 (23)

[a] The numbers in parentheses are the estimated standard deviations. Primed and unprimed atoms are related by the center of inversion.

state. Similar spin mixing has been described for $[Fe(TPP)OClO_3]$[21] and $[Fe(OEP)OClO_3]$.[12,22] In these cases, however, the ground state appears to be predominantly $S = {}^3/_2$ with some $S = {}^5/_2$ character admixed.

(20) Mitra, S.; Date, S. K.; Nipankar, S. V.; Birdy, R.; Girerd, J. J. *Proc. Indian Acad. Sci., Sec. A* **1980**, *89A*, 511–517. The room temperature moment is 5.2 μ_B.

(21) Reed, C. A.; Mashiko, T.; Bentley, S. P.; Kastner, M. E.; Scheidt, W. R.; Spartalian, K.; Lang, G. *J. Am. Chem. Soc.* **1979**, *101*, 2948–2958.

(22) Masuda, H.; Taga, T.; Osaki, K.; Sugimoto, H.; Yoshida, Z.-I.; Ogoshi, H. *Inorg. Chem.* **1980**, *19*, 950–955.

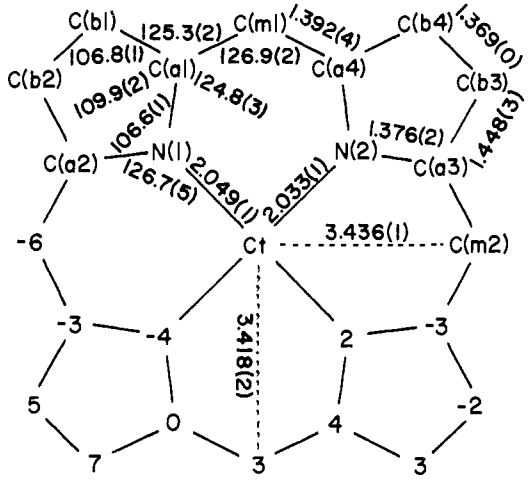

Figure 4. Formal diagram of a porphinato core displaying the average values for the bond parameters. Also displayed are the perpendicular displacements, in units of 0.01 Å, of each of the crystallographically unique atoms from the mean plane of the core. Displacement of the centrosymmetrically related atoms aer equal in magnitude and opposite in sign. The position of the iron atom at the center of the ring has been represented by the symbol Ct.

The structure of the centrosymmetric $[Fe(OEP)(2\text{-}MeIm)_2]^+$ ion and the perchlorate counterion is shown in Figure 3. The figure illustrates the labeling scheme for all unique atoms; these labels are used in all tables. Listings of individual bond distances and bond angles are given in Tables IV and V, respectively. Averaged values for the unique chemical classes of bond distances and angles are entered in the formal diagram of the porphinato core given in Figure 4. Also shown in Figure 4 are the perpendicular displacements of each atom, in units of 0.01 Å, from the mean plane of the core. The deviations from exact planarity are unremarkable as is appropriate for a porphinato complex with a radially expanded core (vide infra).

The geometry of the coordinated imidazole ring is normal. The ring (including the methyl group) is planar to within 0.005 Å. The axial Fe–N bond is tipped by ~3.2° from the normal to the heme plane in such a way as to increase the separation of the C(4) atom from the porphinato core (cf. Figure 4). The unequal Fe–N(3)–C(1) (134.15 (10)°) and Fe–N(3)–C(3) (120.76 (9)°) angles are also important contributors to the increase in the C(4)···core separation. The dihedral angle between the imidazole plane and the mean plane of the metalloporphyrin is 86.1°. The N(4) atom of the 2-methylimidazole is hydrogen bonded to O(1) (O(1)···N(4) = 2.92 Å) or O(2) (O(2)···N(4) = 3.08 Å) depending on the two orientations of the disordered perchlorate anion. The projection of the imidazole plane onto the porphinato plane makes an angle of 22.2° with the N(3)–Fe–N(2) coordinate plane (angle ϕ of Figure 1). Finally, the orientation of the methyl group hydrogen atoms was determined by locating all three hydrogen atoms in difference Fourier maps. All angles subtended at C(4) are within 5° of the ideal tetrahedral values. One hydrogen atom is directed away from the porphinato core (the C–H vector is within 10° of being coplanar with the imidazole plane); the other two hydrogen atoms are correspondingly directed toward the porphinato core. This is illustrated in Figure 1. This is the orientation expected to minimize nonbonded contacts between the methyl hydrogen atoms and core atoms.

The bond distances in the coordination group of $[Fe(OEP)(2\text{-}MeIm)_2]^+$ are $Fe–N_p$ = 2.033 (1) and 2.049 (1) Å and $Fe–N_{ax}$ = 2.275 (1) Å. These values are appropriate[1] for a six-coordinate high-spin iron(III) porphyrinate. The average $Fe–N_p$ bond distance of 2.041 Å is close to the 2.045-Å value found for two[23,24] six-coordinate high-spin iron(III) derivatives having neutral axial ligands. In $[Fe(OEP)(2\text{-}MeIm)_2]^+$, as in the earlier complexes, the porphinato core is radially expanded to accomodate the large iron(III) ion. Values of bond distances in the porphinato core are in accord with this radial expansion. The axial Fe–N(2-MeIm) bond distance of 2.275 (1) Å can be compared with the values observed for low-spin bis(imidazole)iron(III) derivatives: 1.957 (4) and 1.991 (5) Å for $[Fe(TPP)(HIm)_2]^+$,[25] the ~2.01-Å value for $[Fe(OEP)(HIm)_2]^+$,[26] 1.966 (5) and 1.988 (5) Å for $[Fe(PPIX)(1\text{-}MeIm)_2]$,[27] and 2.015 (4) and 2.010 (4) for $[Fe(TPP)(2\text{-}MeIm)_2]ClO_4$.[28] The ~0.30-Å increase in the axial bond distance on changing spin state from low spin to high spin is similar to that observed[7] in the thermal spin-equilibrium form of $[Fe(OEP)(3\text{-}Clpy)_2]ClO_4$. The axial Fe–N(2-MeIm) bond distance can be compared with the 2.316-Å Fe–N(py) distance for the high-spin form[7] of $[Fe(OEP)(3\text{-}Clpy)_2]ClO_4$ and the 2.442 (2) Å found for high-spin [Fe(OEP)(NCS)(py)].[29] The distances are similar to those observed for high-spin $[Fe(TPP)(BzIm)_2]ClO_4$[30] where $Fe–N_p$ = 2.039 (4) and 2.059 (4) Å and Fe–N(BzIm) = 2.216 (5) Å. Interestingly, in both $[Fe(OEP)(2\text{-}MeIm)_2]ClO_4$ and $[Fe(TPP)(BzIm)_2]ClO_4$, the longer $Fe–N_p$ bond is approximately perpendicular to the imidazole plane.

A most interesting comparison of $[Fe(OEP)(2\text{-}MeIm)_2]ClO_4$ is with $[Fe(TPP)(2\text{-}MeIm)_2]ClO_4$.[28] These two species might have been presumed to have been isostructural and to have the same spin state in the solid. However, $[Fe(OEP)(2\text{-}MeIm)_2]ClO_4$ is a near high-spin molecule while $[Fe(TPP)(2\text{-}MeIm)_2]ClO_4$ is a low-spin molecule in the solid; the solid-state coordination group parameters are commensurately different. Nonetheless, in chloroform solution, both species show temperature-dependent magnetic moments suggestive of a $S = {}^1/_2$, $S = {}^5/_2$ spin equilibrium with the low-spin state predominant.[31] The OEP complex has slightly higher moments as would be expected from the effect of porphinato ligand on spin state.[3] The solution magnetic moments demonstrate that the 2-methylimidazole ligand can be a sufficiently strong field ligand to yield low-spin $[Fe(OEP)(2\text{-}MeIm)_2]ClO_4$. Thus, the difference in the solid-state magnetic moments of $[Fe(OEP)(2\text{-}MeIm)_2]ClO_4$ and $[Fe(TPP)(2\text{-}MeIm)_2]ClO_4$ are not an intrinsic feature of the slightly different molecular composition. A consistent explanation of the differing solid- and solution-state magnetic moments for these two species can be given in terms of the orientation of the axial 2-methylimidazole ligands.

We first note that the low-spin bis(unhindered imidazole)iron(III) derivatives previously described[25-27] generally have ϕ values less than 20°.[32] In cases where the two axial imidazoles have different Fe–N bond lengths,[25,27] the longer value is always associated with the imidazole ligand having the smaller ϕ value.[33] The 2-methylimidazole ligand, with its modestly bulky α-methyl

(23) Mashiko, T.; Kastner, M. E.; Spartalian, K.; Scheidt, W. R.; Reed, C. A. *J. Am. Chem. Soc.* **1978**, *100*, 6354–6362.

(24) Scheidt, W. R.; Cohen, I. A.; Kastner, M. E. *Biochemistry* **1979**, *18*, 3546–3552.

(25) Collins, D. M.; Countryman, R.; Hoard, J. L. *J. Am. Chem. Soc.* **1972**, *94*, 2066–2072.

(26) Takenaka, A.; Sasada, Y.; Watanabe, E.; Ogoshi, H.; Yoshida, Z.-I. *Chem. Lett.* **1972**, 1235–1238.

(27) Little, R. G.; Dymock, K. R.; Ibers, J. A. *J. Am. Chem. Soc.* **1975**, *97*, 4532–4539.

(28) Kirner, J. F.; Hoard, J. L.; Reed, C. A. "Abstracts of Papers", 175th National Meeting of the American Chemical Society, Anaheim, CA, March 13–17, 1978; American Chemical Society: Washington, DC, 1978; INOR 14.

(29) Scheidt, W. R.; Lee, Y. J.; Geiger, D. K.; Taylor, K.; Hatano, K. *J. Am. Chem. Soc.* **1982**, *104*, 3367–3374.

(30) Levan, K. R.; Strouse, C. E. "Abstracts of Papers", American Crystallographic Association Summer Meeting, Snowmass, CO, Aug. 1–5, 1983; Abstract H1. Levan, K. R., Ph.D. Thesis, UCLA, 1984.

(31) Solution moments for $[Fe(TPP)(2\text{-}MeIm)_2]ClO_4$: 309 K, 2.73 μ_B; 303 K, 2.69 μ_B; 269 K, 2.60 μ_B; 263 K, 2.64 μ_B; 248 K, 2.55 μ_B (Geiger, D. K., unpublished results). Moments for $[Fe(OEP)(2\text{-}MeIm)_2]ClO_4$: 309 K, 3.45 μ_B; 303 K, 3.22 μ_B; 275 K, 2.83 μ_B; 261 K, 2.75 μ_B; 230 K, 2.63 μ_B.

(32) ϕ values between 0° and 20° are a common feature of five- and six-coordinate imidazole-ligated metalloporphyrins. Kirner, J. F.; Reed, C. A.; Scheidt, W. R. *J. Am. Chem. Soc.* **1977**, *99*, 2557–2563. Scheidt, W. R. *J. Am. Chem. Soc.* **1974**, *96*, 90–94. Dwyer, P. N.; Madura, P.; Scheidt, W. R. *J. Am. Chem. Soc.* **1974**, *96*, 4815–4819. Little, R. G.; Ibers, J. A. *J. Am. Chem. Soc.* **1974**, *96*, 4452–4463.

(33) Although this qualitative statement is always true for a given complex, the ϕ values are not *quantitative* predictors of bond length among the various complexes.

substituent, could be expected to accentuate the required differences in axial bond lengths with changes in the ϕ angle. This appears to be observed in the two complexes at hand. [Fe(TPP)(2-MeIm)$_2$]ClO$_4$ has two independent ligand orientations with ϕ for both $\approx$32°. As noted previously, ϕ for [Fe(OEP)(2-MeIm)$_2$]ClO$_4$ is 22°. Nonbonded contacts between imidazole carbon atoms (both the unsubstituted α-carbon atom and the methyl carbon atom) are relatively short (2.92–3.22 Å) in both species. Surprisingly, perhaps, the shortest nonbonded contact is always between the unsubstituted α-carbon atom, not the methyl carbon atom, and porphinato core atoms. Calculation of H atom···core contacts for both species leads to similar results.[34] The differences in the nonbonded contacts between the two species are only about half of the 0.26-Å difference in axial bond length as a result of the differing orientation of 2-methylimidazole and core conformations. Additional model calculations for [Fe(OEP)(2-MeIm)$_2$]ClO$_4$ with the observed orientation of the 2-MeIm ligand, but with low-spin Fe–N bond distances (2.012 Å), yield shortened H···core contacts of ~2.30 Å. These contacts increase by ~0.10 Å for a 10° rotation of the ligand to ϕ = 32°. We conclude that even a 10° rotation of the axial 2-methylimidazole ligand could be sufficient to require a significant lengthening of the axial bond(s) on the basis of nonbonded packing considerations. These lengthened bonds, in turn, can only be achieved in an intermediate- or high-spin form of the complex.[1] Such bond length–lignad rotation correlations could arise only when the different spin states were energetically similar such as in a spin-equilibrium complex.

The orientation of the axial ligands are, of course, firmly fixed in the solid state. In solution the ligands are freer to rotate around the axial Fe–N bonds.[35] Thus it is reasonable to expect a range of ligand orientations that would allow axial bond elongation and contraction appropriate for the thermal population of the high- and low-spin forms of the molecule. This bond-length variation is not possible in the lattice of [Fe(OEP)(2-MeIm)$_2$]ClO$_4$; the state-dependent magnetic susceptibilities are readily understood as a thermal spin-equilibrium system in solution and a high-spin conformer trapped in the solid state. For [Fe(TPP)(2-MeIm)$_2$]ClO$_4$, the spin equilibrium is shifted more toward the low-spin form in solution and the low-spin state is trapped in the solid. For both species, the solution ground state is low spin.

The foregoing rotational effects are directly applicable to 2-substituted imidazole and unsubstituted pyridine complexes, but not unsubstituted imidazole complexes of unconstrained iron porphyrinates. These effects could be applicable in hemoproteins if the protein could affect both the rotational orientation of the histidine ring and the tilt (nonequal Fe–N–C(α) angles) of the ring. Indeed, such efforts have been suggested as important components of the allosteric mechanism of hemoglobin oxygenation.[36]

Acknowledgment. We thank Professors J. L. Hoard and C. A. Reed for information on [Fe(TPP)(2-MeIm)$_2$]ClO$_4$ in advance of its complete publication. We also thank Prof. C. A. Reed for the SQUID susceptibility measurements, Prof. R. G. Hayes for assistance with EPR measurements, and the National Institutes of Health for support of this work under Grant HL-15627. We thank Prof. K. Hatano for stimulating discussions on bis(imidazole) complexes and Prof. C. E. Strouse for a copy of K. R. Levan's thesis.

Registry No. [Fe(OEP)(2-MeIm)$_2$]ClO$_4$, 92055-42-0; [Fe(OEP)OClO$_3$], 50540-30-2.

Supplementary Material Available: Table II, anisotropic temperature factors, Table III, fixed hydrogen atom coordinates, and listings of the observed and calculated structure amplitudes (×10) for [Fe(OEP)(2-MeIm)$_2$]ClO$_4$ (28 pages). Ordering information is given on any current masthead page.

(34) Calculation of nonbonded distances used the observed methyl group orientation in [Fe(OEP)(2-MeIm)$_2$]ClO$_4$ and an idealized version (C–H vector planar with the imidazole ring) for [Fe(TPP)(2-MeIm)$_2$]ClO$_4$. The C–H distance used was the equilibrium distance of 1.08 Å. The H···core atom distances ranged from 2.55 Å upward for the OEP derivative and 2.41 Å upward for the TPP derivative.

(35) A referee has noted the possibility of an electronic effect on the d-orbital splittings by a ϕ-dependent mixing with the 2-MeIm orbitals. We agree that such an effect is possible and may account for the fact that the observed ϕ values tend to be small values in imidazole-ligated metalloporphyrins. We are inclined to believe that the magnitude of the effect is not sufficient to cause a spin-state change (note, for example, that ϕ ranges from near 0° to 32° in the low-spin bis(imidazole)ferric systems).

(36) Baldwin, J.; Chothia, C. *J. Mol. Biol.* **1979**, *129*, 175–220.

Kinetics of Reversible Intramolecular Elimination Reactions. 1. An Apparent E2 Elimination of a β-Acyloxy Ketone

Barbara J. Mayer,[†‡] Thomas A. Spencer,*[†] and Kay D. Onan[§]

Contribution from the Departments of Chemistry, Dartmouth College, Hanover, New Hampshire 03755, and Northeastern University, Boston, Massachusetts 02115.
Received November 21, 1983

Abstract: The elimination reactions of β-acyloxy ketone **7** and β-acetoxy ketone **1** are both subject to catalysis by hydronium ion, hydroxide ion, and general bases, but the reaction of **7** differs markedly from that of **1**. The reaction of **7** is reversible, and equilibrium amounts of the product enone vary from 16% at pH <3.5 to 100% at pH >7. In addition, **7** reacts from 50 to 10^4 times more rapidly than **1** with basic catalysts ranging in pK_a from 15.7 to 3.3. The Brønsted β for general base catalysis of the E1cB$_I$ reaction of **1** is 0.69, but for the reaction of **7** β = 0.42. That both reactions involve rate-limiting proton removal is evidenced by large invariant primary kinetic isotope effects. These observations lead to the proposal that **7** reacts by an E2 mechanism, previously unobserved in an alkene-forming elimination involving a proton α to a carbonyl group.

Previous studies in this laboratory have shown that the essentially quantitative and irreversible general base catalyzed elimination reactions of **1**, **2**, **3**, and **4** to form enone **5** in aqueous solution proceed by a stepwise mechanism through formation of intermediate enolate anions, **6**.[1-3] Under all conditions used,

[†] Dartmouth College.
[‡] Present address: Department of Chemistry, California State University, Fresno, Fresno, CA 93740.
[§] Northeastern University.

(1) Hupe, D. J.; Kendall, M. C. R.; Spencer, T. A. *J. Am. Chem. Soc.* **1972**, *94*, 1254–1263.

0002-7863/84/1506-6343$01.50/0 © 1984 American Chemical Society